Australian Journal of Basic and Applied Sciences, 5(8): 61-69, 2011
ISSN 1991-8178

Alteration Mapping for Exploration of Porphyry Copper Mineralization in the Sarduiyeh Area, Kerman Province, Iran, Using ASTER SWIR Data

[1]Mohammad Khaleghi, [2]Hojjatollah Ranjbar

[1]Department of Geology, Shahid Bahonar University of Kerman, Iran
[2]Department of Mining Engineering, Shahid Bahonar University of Kerman, Iran

Abstract: The ASTER Shortwave Infra-Red (SWIR) bands, enabled the generation of maps designed to represent the abundance of broad minerals such as kaolinite, muscovite and chlorite which are important in the identification of hydrothermal alterations related to porphyry copper mineralization. SWIR bands from Advanced Space-borne Thermal Emission and Reflection Radiometer (ASTER) with the wavelength between 1.65 and 2.43 µm have a good potential for mapping hydrothermal alteration. In this paper which aims at creating a pixel purity index (PPI), we pre-processed the images with Internal Average Relative Reflectance (IARR)) and used minimum noise fraction (MNF) transformation. PPI was used to extract the most spectrally pure pixels from multispectral images. The study area is located in the south of Kerman city, in southern Iran. Spectral analyses of the hydrothermal alteration minerals of the study area were obtained by matching the unknown spectra of the purest pixel to the U.S Geological Survey (USGS) mineral library. Matched filtering (MF) was used to enhance the hydrothermal alteration minerals of the study area including kaolinite-dickite, muscovite-sericite-illite, and chlorite-epidote by using the spectra which obtained from PPI. We have also used directed principal component analysis (DPCA) for enhancing hydrothermal alteration. Propylitic and phyllic-argillic zones could be separated which are important for porphyry copper exploration.

Key words: ASTER SWIR, Exploration, porphyry copper, Principal Components, PPI, MF

INTRODUCTION

The advanced space-borne Thermal Emission and Reflection Radiometer (ASTER) (Fujisada, 1995; lwasaki *et al.*, 2002) instrument is included on the Earth Observing System (EOS) TERRA platform, and records radiation from the Earth in 14 spectral bands (Table 1). This instrument, providing enhanced capabilities for geological mapping and mineral exploration. The ASTER sensor acquires multi-spectral images. It was loaded onto an EOS terra platform and launched on December 18, 1999 (Rowan and Mars, 2003). ASTER measures reflected radiation in three bands between 0.52 and 0.86 µm (visible and near-infrared (VNIR) region) and in six bands from 1.6 to 2.43 µm (shortwave infrared (SWIR) region), with 15- and 30-m spatial resolution, respectively. In addition emitted radiations are measured at 90-m resolution in five bands in the 8.125-11.65 µm wavelength regions (TIR).

Many of the known porphyry Cu deposits are situated in the Central Iranian Volcanic Belt. This belt has a great potential as far as Tertiary porphyry copper mineralization is concerned. Given the poor soil development, relatively poor vegetation cover but abundant outcrops the arid/semiarid part of the belt is suitable for remote sensing studies. Hydrothermally altered rocks have received considerable attention because of their potential economic implications and favorable spectral characteristics for remote identification (Rowan *et al.*, 2003; Abrams *et al.*, 1977, 1983; Goetz *et al.*, 1983; Podwysocki *et al.*, 1983; Kruse *et al.*, 1993; Crosta *et al.*, 2003; Galvao *et al.*, 2005).

Phyllic, argillic and potassic zones are associated with hydrothermal alterations in porphyry type deposits. An oxide zone is developing over many of the porphyry bodies, which are rich in iron oxide minerals (Azizi *et al.*, 2010). Landsat data has been used for a number of years in arid and semi-arid environments to locate areas of iron oxides and/or hydrous minerals (Abrams *et al.*, 1983; Kaufman, 1988 and Tangestani and Moore, 2001) which may be associated with hydrothermal alteration zones. Host rocks that contain ore deposits of hydrothermal origin always show the results of the interaction with the hydrothermal fluids that changed the mineral and chemical composition of the rock and caused the deposition of the ore and related hydrothermal

Corresponding Author: Mohammad Khaleghi, Department of Geology, Shahid Bahonar University of Kerman,
E-mail:mohammadkhaleghi1984@Gmail.com

minerals (Rutz-Armenta, J.R. and Prol-Ledesma, R.M., 1998). Tommaso and Rubinstein (2007) did hydrothermal alteration mapping using ASTER data in the Infiernillo porphyry deposit, Argentina. Azizi *et al.* (2010) extracted hydrothermal alterations from ASTER SWIR data from east Zanjan area, northern Iran. Hosseinjani and Tangestani (2011) have used mixture tuned matched filtering (MTMF) for alteration mapping in Sarduiyeh area.

The aim of this paper is to enhance the minerals of argillic, phyllic and propylitic alterations related to the copper porphyry deposit of the study area using the spectra obtained by PPI method through matched filtering (MF) and directed principal component analysis.

Table 1:. Wavelength ranges and spectral resolution of ASTER bands (Abrams, 2000).

	VNIR	SWIR	TIR
Spectral bandwidth (μm)	Band 1 0.52–0.60	Band 4 1.650–1.700	Band 10 8.125–8.475
	Band 2 0.63–0.69	Band 5 2.145–2.185	Band 11 8.475–8.825
	Band 3 N 0.78–0.86	Band 6 2.185–2.225	Band 12 8.925–9.275
	Band 3B 0.78–0.86	Band 7 2.235–2.285	Band 13 10.25–10.95
	(backward looking)	Band 8 2.295–2.395	Band 14 10.95–11.65
		Band 9 2.360–2.430	
Spatial resolution (m)	15	30	90

Geological Setting:

The study area (E57°00´-57°30´ and N29°00´-29°15´) is located in the southern part of Central Iranian Volcano- Sedimentary complex (Urumiyeh-Dokhtar belt), south-southeast of Kerman province (Fig. 1). The mentioned area is located in the southern part of Dehej-sarduiyeh volcanic belt (Fig. 2).

Fig. 1: Sketch map showing the position of the Central Iranian Volcanic Belt and porphyry-type Cu deposits sub-parallel to the Zagros Thrust Zone (Shahabpour, 1994). 1 – Bahreasman; 2 – Takht; 3 – Kuhe Panj; 4 – Darehezar; 5 – Sar Cheshme; 6 – Meiduk; 7 – Gowde kolvary; 8 – Darre Zereshg; 9 – Southest of Ardestan; 10 – Sharif Abad; 11– songun (modified from Shahabpour, 1994).

This area is recognized by its Eocene volcano-sedimentary complex which is one of the most astonishing geological formations in Kerman province (shahabpour, 1994). This belt is also a massive source of copper in the area.

The most impressive geological feature in study area is the Eocene sequences, consisting of andesite, andesite-basalt, basalt, rhyolite, trachyte, trachyandesite, trachybasalt and pyroclastics. The oldest geological unit in the area is the colored mélange unit which has an upper Cretaceous age. Argillization, sericitization, propylitization and silicifiction are the most common types of hydrothermal alterations in the area (Geological Survey of Iran 1973). Copper occurrence are numerous, some of them being exploited in the ancient times. There are several ore indications and mineralization such as Hosseyn Abad, Qanat Darreh, Dolat abad, Zamin Hossein, and Sarduiyeh-Hanzakoyeh in the study area, which is why aforementioned area was chosen for remote sensing studies.

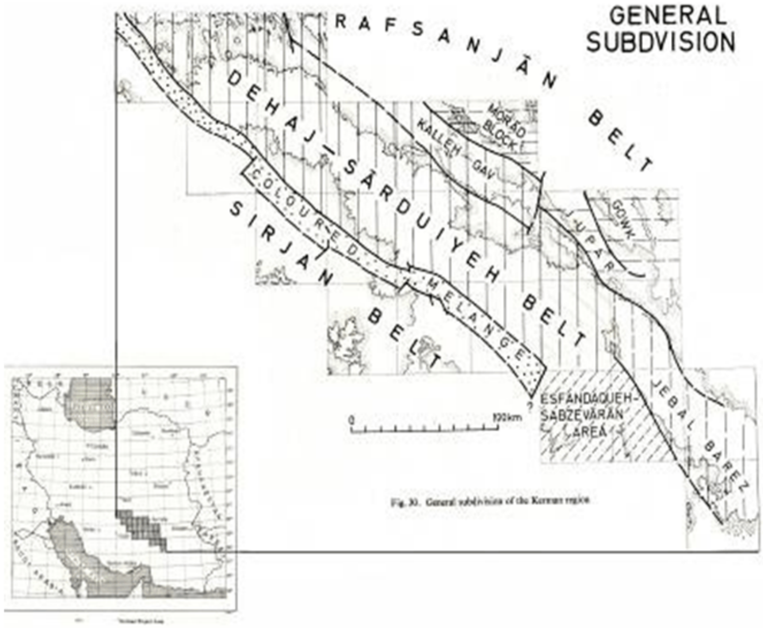

Fig. 2: Gological setting: Dehej-Sarduiyeh Belt (Geological Survey of Iran 1973).

Data Processing:

Many image analysis and processing techniques can be used to interpret the remote sensing spectral data. Band ratio, Principal component analysis (PCA), Minimum noise fraction (MNF), spectral angle mapper (SAM) and Linear Spectral Unmixing (LSU) are important techniques that are used for finding alteration zones. In this research, we used several methods including DOCA, MNF, PPI, and MF for the discrimination of alteration zones.

Directed Principal Component Analysis:

Principal component analysis (PCA) determines the eigenvectors of a variance-covariance or a correlation matrix. The resulting components are often more interpretable than the original images. PCA is widely used for alteration mapping in metallogenic provinces (e.g., Crosta and Moore, Tanagestani and Moore, 2001; Crosta *et al*., 2003). PCA can be applied to multivariate datasets, such as multispectral remote sensing images, with the purpose of highlighting spectral responses related to specific hydrothermal alteration minerals (Crosta *et al*., 2003). In the directed PCA analysis only certain bands are chosen that contain absorption and reflection features of the minerals under investigation. If the number of input channels is reduced to avoid a particular spectral contrast, the chances of defining a unique principal component for a specific mineral class will be increased (Ruiz-Armenta and Prol-Ledesma, 1998).

Directed PCA technique has been applied in this study. An approach based on the examination of eigenvector loadings in each PC image is used for determining which image contains information related to the spectral signatures of specific target minerals. It is expected that the PC image that collects moderate to high eigenvector loadings for the diagnostic absorptive and reflective bands of the index mineral could be considered as the specific image for that mineral. If the loading of absorptive band is negative in sign, the target area will be enhanced in bright pixels, and if the loading of reflective band is negative, the area will be enhanced in dark pixels (Crosta and Moore, 1989).

Table 2 shows the eigenvector loadings for bands 4, 6 and 7. As phyllic alteration has an absorption in band 6, and reflections in bands 4 and 7, PC3 can show the areas with phyllic alteration (Fig. 3). Table 3 shows the eigenvector loadings for bands 4, 5 and 7. As argillic alteration has an absorption in band 5, and reflections in bands 4 and 7, PC3 can show the areas with argillic alteration (Fig. 4). Comparison of figures 3 and 4 shows that the areas of phyllic and argillic alterations are almost overlapping. Table 4 shows the eigenvector loadings for bands 7, 8 and 9. As propylitic alteration has an absorption in band 8, and reflections in bands 7 and 9, PC3 can show the areas with propylitic alteration. The inverse of this PC is used for enhancing propylitic areas with white pixels (Fig. 5).

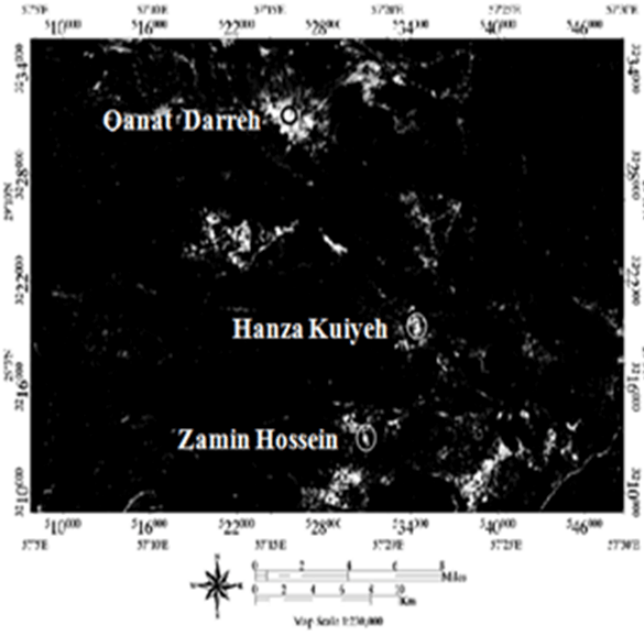

Fig. 3: The phyllic image that is prepared based on the eigenvector loadings (PC3) of table 2.

Table 2: The result of DPCA for enhancing phyllic zone.

	Pc1	Pc2	Pc3
Band 4	0.62	0.78	0.02
Band 6	0.54	- 0.41	- 0.72
Band 7	0.55	- 0.46	0.68
Eigen value	0.107282	0.001374	0.000402

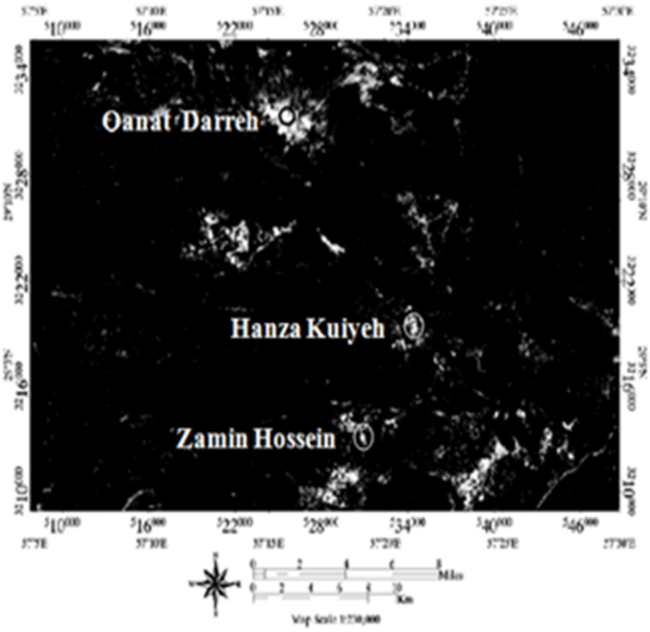

Fig. 4. The argillic image that is prepared based on the eigenvector loadings (PC3) of table 3.

Table 3:. The result of DPCA for enhancing argillic zone.

	Pc1	Pc2	Pc3
Band 4	0.63	0.77	0.05
Band 5	0.53	- 0.37	- 0.75
Band 7	0.56	- 0.5	0.64
Eigen value	0.107282	0.001374	0.000402

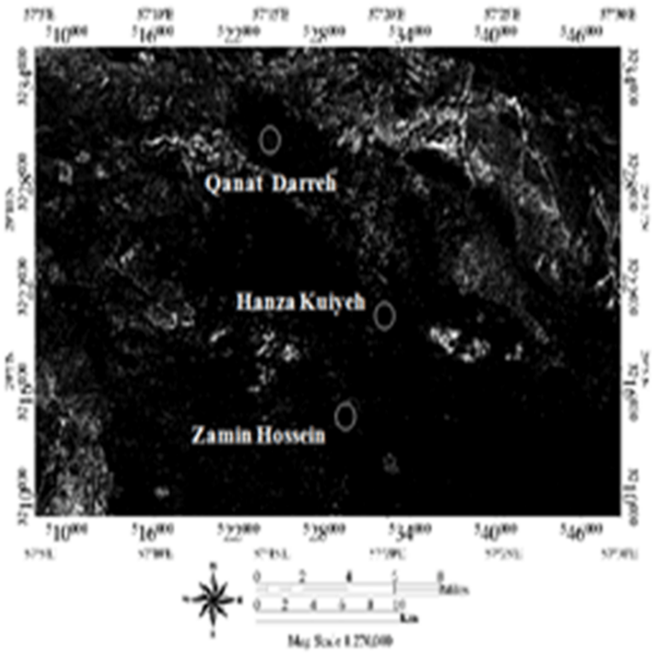

Fig. 5: The propylitic image that is prepared based on the eigenvector loadings (PC3) of table 4.

Table 4: The result of DPCA for enhancing propylitic zone.

	Pc1	Pc2	Pc3
Band 7	0.58	0.43	- 0.63
Band 8	0.60	0.33	0.72
Band 9	0.54	- 0.83	- 0.62
Eigen value	0.098944	0.000493	0.000320

Minimum Noise Fraction (MNF) Method:

MNF analysis identifies the location of spectral signature anomalies. This process is of interest to the mineral exploration communities because spectral anomalies are often indicative of alterations. MNF transform is used to determine the inherent dimensionality of image data to segregate noise in the data and to reduce the computational requirements for subsequent processing (Boardman and kruse, 1994). This method is similar to principal component (PC) analyses that have been used for a long time in multispectral image processing but involves an extra preceding step. MNF is used as a preparatory transformation to condense most of the essential components into a few spectral bands. The first MNF bands contain signal and the remaining bands contain noise (Altinbas *et al.*, 2004).

Pixel Purity Index (PPI) and Extracted End-member Spectra:

The PPI function which stands for the pixel purity index is used to automatically locate the pixels with the highest level of spectral purity in higher order MNF eigen-images which are multispectral and hyperspectral data (Boardman, 1993). N-Dimensional scatter plots are repeatedly projected onto a random unit vector in order to calculate the pixel purity index. The most spectrally pure or extreme pixel corresponds to materials with spectra that create the spectra through linear combination. A pixel purity image, in which the digital number (DN) of each pixel corresponds to the number of times that pixel was recorded as extreme, is created after the total number of times each pixel is marked as is every projection is noted.

As mentioned earlier the PPI function is performed using MNF images. The threshold factor of 2.5 was used with 10000 iterations in order to locate the purest pixels. High-DN pixels or pure pixels were determined through the use of density slice thresholds. These values were applied to compute the region of interest (ROI), being used for n-dimensional visualization. The purest pixels are located, identified and clustered using n-dimensional visualization in conjunction with the MNF and PPI results.

The most extreme spectral responses are also found using the same method in data set. In this study, pure pixels were extracted by performing the n-dimensional visualization on the MNF images. After finding the pure pixels, their spectra were determined, and six types of classes were extracted.

In order to derive these spectra from the Internal Average Relative Reflection (IARR) images, spatial locations of the pixels were taken from MNF image through the inversion of the MNF plots to the spectra. Further processing was performed by using the extracted spectra as references.

Matching Class Spectra to Library Spectra and Mapping Classes:

The USGS mineral library was used to perform the matching process. Spectral analysis was used to create a score between 0 and 1, where the value of 1 demonstrates a perfect match, and to identify mineral types. It is well known that certain minerals are similar in a particular wavelength ranges. To obtain the best possible results, a wavelength range that contains diagnostic absorption features was used to distinguish among the minerals (Fig 6). Table 5 indicates the ranked score or weighted score for each of the classes in the input spectral library which are obtained through spectral analysis. The highest score represent the closest match and a higher confidence in the degree of spectral similarity. The spectra so obtained were used in MF for alteration mapping.

Table 5: Score of the extracted spectra

Spectral class	Mineral type	Score between 0 and 1
Class#1	Illite	0.966
Class#2	Muscovite	0.998
Class#3	Kaolinite	0.943
Class#4	Dickite	0.952
Class#5	Epidote	0.966
Class#6	Chlorite	0.900

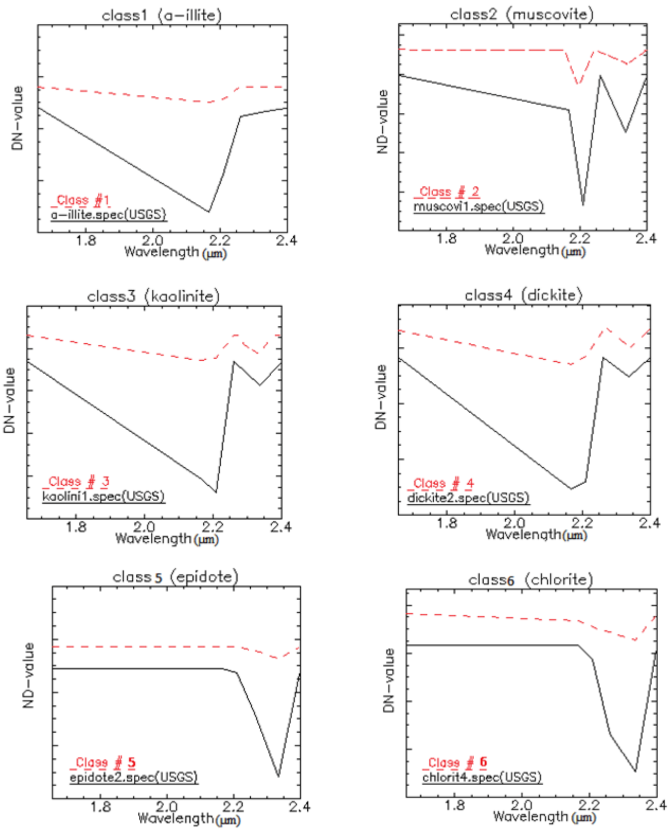

Fig. 6: Matching class spectra to USGS mineral spectral library.

Matched Filtering (MF):

Matched filtering performs partial unmixing. This technique only finds the user defined endmember because not all the endmembers need to be known. This method maximizes the known endmember's response and suppresses the response of the unknown composite background. It does not require knowledge of all endmember within an image and detected alteration minerals including kaolinite, muscovite and epidote-chlorite based on matches to extracted endmember spectra which are obtained through PPI that scored by spectral analysis (Fig. 7). In all the images the sedimentary rocks and vegetation cover are masked.

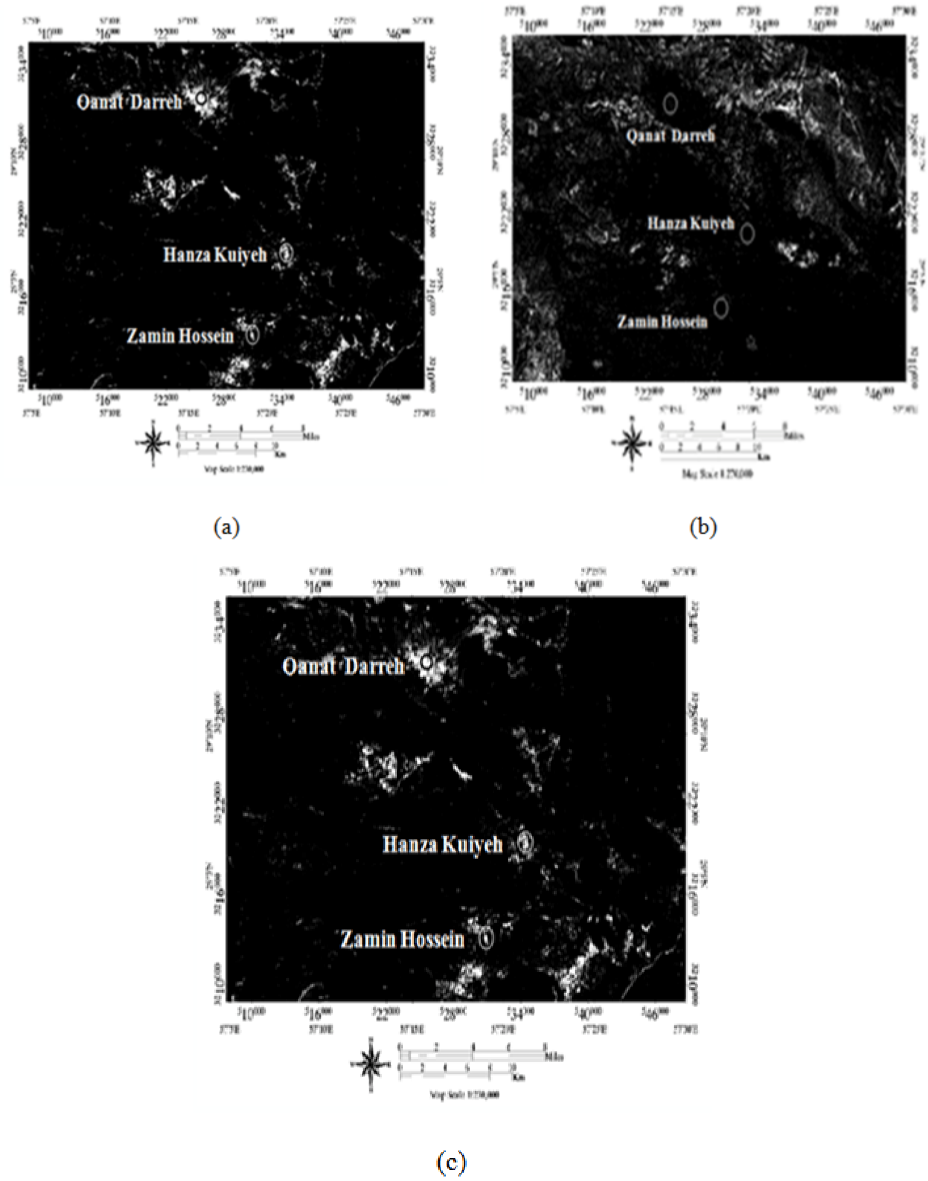

Fig. 7: Haydrothermal alterations are enhanced using MF; (a) Phyllic, (b) Propylitic, (C) Argillic.

Discussion and Conclusion:

In order to check the accuracy of results, the altered areas and the reported mineralized areas were visited for ground control and sampling. The procedure at each station included field observations, GPS readings, collection of samples for chemical analysis, petrography and XRD analysis and taking field photographs.

Hydrothermal alterations related to porphyry copper deposits and mineralization in the studied area such as Zamin Hosseyn, Qanat Darreh and Hanza kuiyeh were mapped Using the SWIR ASTER data and image processing methods such as PPI, MF and DPCA. PPI technique used for obtaining the pure pixels and extracting the endmember spectra with the best matching to USGS spectral library, which was performed with the use of spectral analysis scoring system. The extracted spectra so obtained were used in the MF method and hydrothermal alteration such as Phyllic, propylitic and argillic were enhanced. There is a good correspondence between the copper mineralization and the argillic-phyllic altered areas mapped by MF and DPCA methods.

Comparison of the DPCA and MF results with the results obtained from ground samples shows that both methods could enhance the altered areas. Although MF gave a better result. The argillic zone due to its spectral similarities with the phyllic zone in terms of absorptions and reflection bands is difficult to enhance well by ASTER data. The similarities between the phyllic and argillic images obtained by MF and DPCA can be attributed to the surface weathering and formation of clay minerals over the phyllic altered zones.

REFERENCES

Abrams, M.J., 2000. The advanced spaceborne thermal emission and reflection radiometer (ASTER): data products for the high spatial resolution imager on NASA Teraa Platform. International Journal Of Remote Sensing, 21: 847-859.

Abrams, M.J., *et al.,* 1977. Mapping of hydrothermal alteration in Cuprite mining district, Nevada, Using aircraft scanner images for the spectral region 0.46 to 2.34 mm. Economic Geology, 98: 1019-1027.

Abrams, M.J., *et al.*, 1983. Remote Sensing of porphyry copper in Southern Arizona. Economic Geology, 78: 591-604.

Altinbas, U., *et al.*, 2004. Using advanced spectral analysis techniques as possible means of identifying clay minerals. Turkish Journal of Agriculture, 29: 19-28.

Azizi, H., *et al.*, 2010. Extraction of hydrothermal alteration from ASTER SWIR data from east Zanjan, northen Iran. Advances in Space Research, 46: 99-109.

Boardman, J.W., 1993. Automating spectral unmixing of AVIRIS data using convex geometry concepts. In: Summaries of the 4th Annual JPL Air-borne Geoscience Workshop, Pasadana, 11-14.

Boardman, J.W. and F.A. Kruse, 1994. Automated spectral analysis: A geological example using AVIRIS data, Northern Grapevine Mountains, Nevada: In Proceeding Tenth Thematic Conference. Geological Remote Sensing, 9-12 May, San Antonio, Texas, 407-418.

Crosta, A.P. and J.M. Moore, 1989. Enhancement of Landsat Thematic Mapper imagery for residual soil mapping in SW Minais Gerais State, Brazil: a prospecting case history in Greenstone Belt Terrain. In *Proceedings of the Seventh Thematic Conference on Remote Sensing for Exploration Geology*, 2- 6 October, Calgary, Canada, Environmental Research Institute of Michigan, pp: 1173-1187.

Crosta, A.P., *et al.,* 2003. Alteration minerals in epithermal deposits in Patagonia, Argentina, Using ASTER imagery and principal component analysis. International Journal Of Remote Sensing, 24: 4233-4240.

Fujisada, H., 1995. Design and performance of ASTER instrument, Proceeding of International Society for Optical Engineering, 16-25.

Galvao, L.S., *et al.*, 2005. Use of ASTER short-wave infrared bands for the spectral discrimination of hydrothermal altered materials: Central Mexico. International Journal Of Remote Sensing, 1: 3 -15.

Geological Survey of Iran, 1972. Geological map of Sarduiyeh 1:100000 SHEET 7447.

Geological Survey of Iran, 1973. *Exploration for ore deposits in Kerman region*. Geological Survey of Iran publication, Tehran. Report No. 53.

Goetz, A.F.H., B.N. Rock, L.C. Rowan, 1983. Remote sensing for exploration , an overview. Economic Geology, 78: 573-590.

Hosseinjani, M. and M.H. Tangestani, 2011. Mapping alteration minerals using sub-pixel unmixing of ASTER data in the Sarduiyeh area, SE Kerman, Iran. International Journal of Digital Earth, 1: 1-18.

Kaufman, H., 1988. Mineral exploration along the Agaba-Levant structure by use of TM-data concepts, processing and results. International Journal Of Remote Sensing, 9: 1630-1658.

Kruse, F.A., *et al.*, 1993. The spectral image processing System (SIPS) – interactive visualization and analysis of imaging spectrometer data. Remote Sensing of Enviroment, 44: 145-163.

Lwasaki, A., H. Fujisada, H. Akao, O. Shindou and S. Akagi, 2002. Enhancement of spectral separation performance of ASTER/SWIR, in: Strojnik, M., and Anderson, B., eds., Proceeding of International Society for Optical Engineering, 42-50.

Podwysocki, M.H., *et al.*, 1983.Use of multispectral images for assessment of hydrothermal alteration in the Marysvale, Utah, mining area. Economic Geology, 78: 675-678.

Rowan, L.C. and J.C. Mars, 2003. Lithologic mapping in the Mountain Pass, California area using Advanced Spaceborne Thermal Emission and Reflection Radiometer (ASTER) data. Remote Sensing of Environment, 84: 350-366.

Rowan, L.C., *et al.*, 2003. Mapping hydrothermally altered rocks at the Cuprite Nevada using the advanced spaceborne thermal emission and reflection radiometer (ASTER), a new satellite-imaging system. Economic Geology, 98: 1019-1027.

Ruiz-Armenta, J.R. and R.M. Prol-ledsma, 1998. Techniques for enhancing the spectral response of hydrothermal alteration minerals in Thematic Mapper images of Central Mexico. International Journal of Remote sensing, 19: 1981-2000.

Shahabpour, J., 1994. Post mineralization breccias dike from the Sar Cheshme porphyry copper deposit, Kerman, Iran. Exploration and Mining Geology, 3: 39-43.

Tangestani, M.H., and F. Moor, 2001. Comparison of three principal component analysis techniques to porphyry copper alteration mapping: A case study, Meiduk area, Kerman, Iran, Canadidan Journal of remote sensing, 27: 176-181.

Tommaso, I., N. Rubinstein, 2007. Hydrothermal alteration mapping using ASTER data in the infiernillo porphyry deposit, Argentina. Ore geology Reviews, 32: 275-290.